

Stress-Strain State of Flexible Double-Layer Reinforced Cement Elements with Fireproofing Vermiculite Concrete Layer

Zhurtov A.V.

Institute of Architecture, Construction and Design
Kabardino-Balkarian State University
named after H.M. Berbekov
Nalchik, Russia
zhurtovartur@mail.ru

Khezhev T. A.

Institute of Architecture, Construction and Design
Kabardino-Balkarian State University
named after H.M. Berbekov
Nalchik, Russia
hejev_tolya@mail.ru

Kokoev M. N.

Institute of Architecture, Construction and Design
Kabardino-Balkarian State University named after H.M. Berbekov
Nalchik, Russia
kbagrostroy@yandex.ru

Abstract – There is the study outcome of the stress-strain state of single-layer and double-layer reinforced concrete elements with simple bending in the article. The data obtained in numerical experiments on finite element schemes perfectly matches the field tests results.

Keywords – stress-strain state of reinforced concrete elements; concrete; vermiculite concrete; fireproof.

I. INTRODUCTION

Today, the construction industry development is characterized by an increase in number of storeys in the building and structures, an increase in the length of escape routes, and the use of long-span thin-walled reinforced concrete and reinforced concrete structures, which requires effective fire safety and fire resistance measures for building structures.

The most effective measure that increases steel and reinforced concrete structures fire resistance is the protection of structures with thermal insulation materials.

For building structures' fireproof, heat-insulating materials are used in the form of cladding of slab, sheet, piece products, as well as plasters.

The application of this fireproofing method for thin-walled steel and reinforced concrete structures can be effective while performing heat-shielding and acoustic functions.

Fire resistant plasters based on expanded vermiculite 15–20 mm thick and weighing 9–12 kg per 1 m² do not lead to significant elements weighting, having a mass of about 60–70 kg per 1 m², and at the same time provide a sufficient fire resistance.

Vermiculite has such properties as a high sound absorption coefficient, a pleasant color (golden or silver) fire retardant coating along with the main function – fire protection. Therefore, it can significantly improve the acoustic and decorative characteristics of reinforced concrete constructions. This is very important for hall rooms where doubly curved shell implementation is limited due to insufficiently high acoustic characteristics. In addition, concrete-vermiculite solutions have good thermal insulation properties [1-3].

In studies [4–5], in order to increase the reinforced concrete structures' fireproofing limit, a method for manufacturing double-layer reinforced concrete elements with a fire-retardant layer of vermiculite concrete in a single technological process was proposed. This allows ensuring reliable operation of the constructive and flame retardant layers both at normal temperatures and when exposed to high temperatures during a fire. The purpose of the study is to examine the stress-strain state of single-layer and double-layer reinforced concrete elements with simple bending.

II. METHODS AND MATERIALS

For the reinforced concrete layer, sand with a fineness modulus of 2.37 was used, with a maximum grain size of 5.0 mm. Fine-grained concrete mixture was used in the composition C : S = 1: 2.5 with a W / C = 0.4 ($R_{compress.} = 55$ MPa, $R_{bend} = 6.5$ MPa).

For the samples reinforcement, a woven mesh No. 8 with a diameter of 0.7 mm was used in accordance with GOST 3826–82.

For vermiculite concrete layer, expanded vermiculite from the Kovdor field with a maximum grain size of 5.0 mm was

used, composition C: vermiculite = 1: 3 (by volume), W / C = 1.25 ($\rho = 640 \text{ kg / m}^3$, $R_{compress.} = 2.3 \text{ MPa}$, $R_{bend} = 1.3 \text{ MPa}$).

Portland cement of the grade PC 500-DO from the Volkhov plant (table 1) was used as a binder for vermiculite concrete. When choosing a binder for vermiculite concrete, it was assumed that the vermiculite concrete mixture and the fine-grained concrete mix of the concrete layer will be subjected to the same technological redistribution in the double-layer reinforced concrete structures manufacture process. High-grade Portland cement use will provide vermiculite concrete with an improved form-flattening strength, which is very important for concrete with a lower average density and low strength.

Chemical compositions of materials used in research for vermiculite concrete and fine-grained cement-reinforced structures' concrete are given in Table. 2, granulometric - vermiculite and sand – in tTable. 3.

The manufacture of boards with a size of $2000 \times 500 \text{ mm}$ was produced in a laboratory installation by the method of vibroforming. The shaping of the vermiculite concrete layer was accomplished from below or above the reinforced concrete layer. The mixing zone between the layers was 2–3 mm. Samples with dimensions of $400 \times 100 \text{ mm}$ for tests on simple bending were cut from the board.

To assess the double-layer cement-reinforcing elements' stress-strain state, as well as to analyze the joint fireproofing and structural concrete layers, 4 series of samples (Fig. 1) $100 \times 400 \text{ mm}$ in size, differing in manufacturing method, thickness of vermiculite concrete layer, and steel woven meshes number and location, were tested for bending. The bending test also evaluated the effect of the vermiculite concrete layer on the strength, stiffness and crack resistance of bent elements.

TABLE I. PHYSICAL AND MECHANICAL PERFORMANCE OF PORTLAND CEMENT

Standard consistency of hydrated cement, %	Time of initial setting, min	Time of final setting, min	brand of cement
27.8	130	350	500

TABLE II. CHEMICAL COMPOSITION OF MATERIALS

Material item	SiO ₂	Al ₂ O ₃	Fe ₂ O ₃	CaO	MgO	SO ₃	K ₂ O+Na ₂ O	loss on imination
Portland cement	21.4	4.2	4.3	61.2	2.9	2.4	1.6	2.3
Ash	58.7	17.6	7.7	5.7	2.9	0.4	4.4	2.0

TABLE III. AGGREGATE GRAIN-SIZE DISTRIBUTION

Material item	Partial residuals on the mash screens, %					Passed through the sieve 0,14
	2,5	1,25	0,63	0,315	0,14	
Sand	7.1	12.8	26.4	98.7	21.1	3.9
Vermiculite	26.0	21.3	30.6	14.4	5.1	2.6

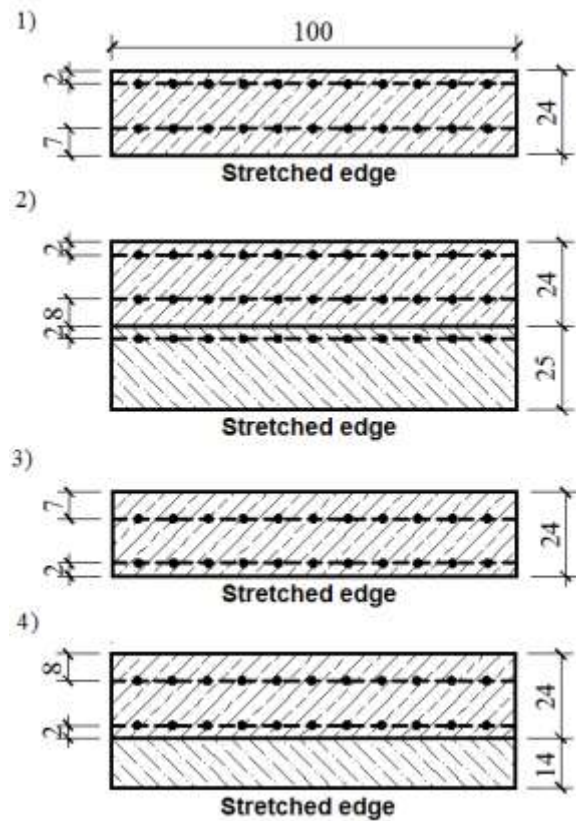


Fig. 1. Schemes of single-layer (1, 3) and double-layer samples reinforcement with vermiculite concrete layer (2, 4).

The loading of samples was of a short-term nature and was carried out through a special device with unit loads. To monitor the deformations, displacements and the process of cracking tensiometers (LC) with a base of 50 mm; displacement indicating gage (DI); BCH-2 microscope with a 24-fold increase and measuring sensitivity of 0.05 mm. were used.

Samples at the age of one month were tested for bending. The test was carried out according to the scheme of simple bending in a flat position with the location of the vermiculite concrete layer in the stretched zone, the span between opars was 300 mm (Fig. 2). Three samples were tested in each series.

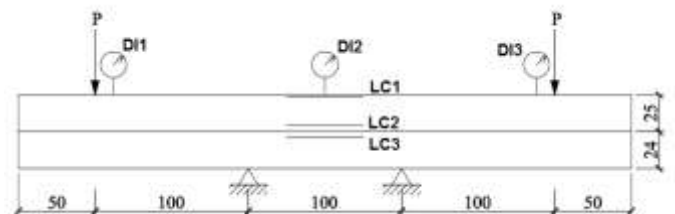


Fig. 2. The scheme of series No. 2 testing samples with a simple bend.

III. RESULTS

During the samples testing using a microscope, it was not possible to detect cracks in single-layer reinforced concrete

samples, however, tensiometers recorded relative deformations of $35 \cdot 10^{-5}$ at the time preceding failure.

When testing double-layer samples, the first cracks in the vermiculite concrete layer with an opening width of 0.01–0.02 mm were found with bending moments of 5–6 kN · cm, which is not incommensurate with the destructive ones for single-layer samples. The maximum crack opening width at the moment preceding the destruction was 0.03–0.05 mm. The number of cracks ranged from 4 to 7. Some cracks spread along the height of the vermiculite concrete layer to 10–15 mm by the time preceding the destruction. No cracks were found in the effective reinforced concrete layer area in the double-layer samples.

At loads ($M = 5–6 \text{ kN} \cdot \text{cm}$), corresponding to destructive for single-layer samples, the deformations measured in double-layer samples in the transition zone of the cement-reinforced layer to vermiculite concrete were $10–15 \cdot 10^{-5}$. This indicates that the vermiculite concrete layer significantly increases the single-layer cement-reinforced samples stiffness. At the preceding the destruction moment, the bending moment was 9.5 kN · cm for double-layer samples of the second and fourth series, respectively.

Higher unit strain of second series' samples compared with samples of the fourth series are explained by an additional woven mesh in the vermiculite concrete layer, which is used for technological purposes.

Up to a bending moment of 650–700 kgf · cm, the relative deformations measured in double-layer reinforced concrete samples in the cement-layer transition zone to the vermiculite-concrete layer are 1.5–3.5 times less than the deformations of effective concrete single-layer samples area.

A further increase in the load leads to a rapid increase in the unit strain of effective concrete double-layer samples area towards the single-layer samples. This is explained by the fact that when the values of the bending moment are more than 650 kgf · cm, the vermiculite concrete layer begins to be turned off from the operation of double layer samples.

The study of the nature of the cracks transition from the reinforced concrete layer to the vermiculite concrete and vice versa is interesting, since vermiculite concrete has a relatively low modulus of elasticity $E = 3.5–5.0 \cdot 10^3 \text{ MPa}$. Moreover, a fine-mesh woven mesh in a vermiculite concrete layer at the boundary of the layers means certain changes in the process of cracking.

It should be noted that during the double-layer reinforced concrete samples testing, no adhesion failure of the layers, detachments of the vermiculite concrete layer from the reinforced concrete layer was detected.

Thus, until the formation of cracks with an opening width of 0.05–0.1 mm in single-layer cement-reinforcing samples, an additional fireproofing layer significantly increases their crack resistance.

The results of testing all four series samples are shown in Fig. 3.

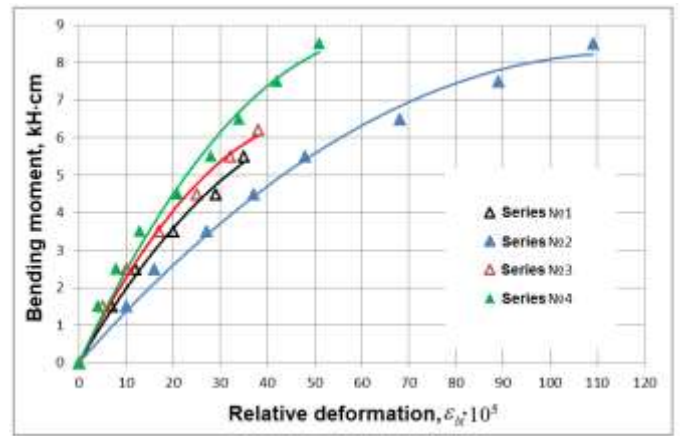


Fig. 3. Deformations of the samples' effective area (average for the zone of pure bending).

The nonlinear nature of the diagrams of the bending moment dependence on the effective area unit strain emphasizes that the plastic properties of materials, as well as the elastic properties of concrete and reinforcing mesh, should be taken into account in the double-layer element operating. Also, the graphs' nonlinear nature indicates a gradual development of cracks, and consequently, the stretched concrete layers with cracks are gradually removed from operating, which leads to a gradual decrease in the stiffness of the sample cross section [6–8].

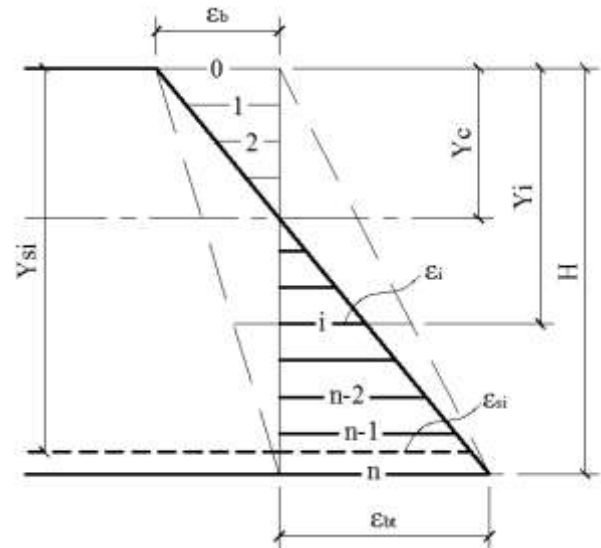


Fig. 4. Scheme to define the deformations in the normal section.

To analyze the stress-strain state of single-layer and double-layer samples' cross sections with simple bending, the so-called "deformation model" section was used. This method is based on deformation diagrams that describe the concrete and reinforcement non-linear operation, and some law of the unit strain distribution over the cross-sectional elements' area: here the plane-sections hypothesis was used. The "stress – unit strain" dependence of a curvilinear type, constructed according to the N.I. Karpenko, was used as a diagram of the materials

deformation [9–11]. In contrast to the method of limiting efforts, the “deformation model” allows analyzing the cross-sections not only in the limiting, but also in the pre-limiting and over-limiting states. However, the use of the “deformation model” requires a numerical method for solving the nonlinear problem of calculating normal sections.

To solve the nonlinear problem of calculating normal sections, the following method is proposed. The section is divided in height into n-number of small-area finite elements (Fig. 4).

At that, from the plane-sections hypothesis it follows:

$$\left\{ \begin{aligned} \varepsilon_i &= \varepsilon_{bt} \cdot \left(\frac{i}{n}\right) - \varepsilon_b \cdot \left(\frac{n-i}{n}\right); \\ \varepsilon_b &= \frac{Y_c}{h - Y_c} \cdot \varepsilon_{bt}; \\ \varepsilon_{sj} &= \frac{Y_{sj} - Y_c}{h - Y_c} \cdot \varepsilon_{bt}. \end{aligned} \right.$$

where

$\varepsilon_b, \varepsilon_{bt}, \varepsilon_i, \varepsilon_{sj}$ – respectively, the relative deformation of compressed, stretched, *i*-th fiber of concrete and the *i*-th reinforcing mesh;

Y_{si} – the distance from the gravity center of the reinforcement mesh to the element’s effective area;

Y_c – the distance from the element’s effective area to the neutral axis of the cross section;

h – element depth of section;

n – number of finite elements.

Let us express the the *i*-th fiber section unit strain through the effective area deformation by the formula

$$\varepsilon_i = \frac{Y_c - Y_i}{h - Y_c} \cdot \varepsilon_{bt} = \frac{Y_c - \left(\frac{i \cdot h}{n}\right)}{h - Y_c} \cdot \varepsilon_{bt}, \quad i = 0, 1, 2, \dots, n.$$

Using the analytical dependence of the secant modulus of concrete deformation on the unit strain $f(\varepsilon)$, it is possible to determine the stress σ_i arising in the *i*-th final section element and the stress σ_{sj} arising in the *i*-th woven mesh using the formula

$$\sigma_i = \frac{\sigma_{i-1} + \sigma_i}{2} = \frac{\varepsilon_{i-1} \cdot f(\varepsilon_{i-1}) + \varepsilon_i \cdot f(\varepsilon_i)}{2}, \quad i = 1, 2, \dots, n,$$

$$\sigma_{sj} = E_s \cdot \varepsilon_{sj}, \quad j = 1, 2, \dots, k,$$

where

$$f(\varepsilon_i) = E_{b0} \cdot v_b(\varepsilon_i),$$

E_{b0} – tangent modulus of concrete elasticity in compression,

v_b – the variation coefficient of the secant modulus of deformation under compression, can be determined by the formula

$$\left\{ \begin{aligned} v_b(\varepsilon_i) &= p + \sqrt{p^2 + s}; \\ p &= \frac{\hat{v}_b \cdot [2 \cdot \hat{v}_b^2 - \omega_1 \cdot \eta_d \cdot (v_0 - \hat{v}_b)^2]}{2 \cdot [\hat{v}_b^2 + \omega_2 \cdot \eta_d^2 \cdot (v_0 - \hat{v}_b)^2]}; \\ s &= \frac{\hat{v}_b^2 \cdot (v_0^2 - 2 \cdot v_0 \cdot \hat{v}_b)}{\hat{v}_b^2 + \omega_2 \cdot \eta_d^2 \cdot (v_0 - \hat{v}_b)^2}; \end{aligned} \right.$$

where

$$\omega_1 = 2 - 2,5 \cdot \hat{v}_b(t);$$

$$\omega_2 = 1 - \omega_1 = 2,5 \cdot \hat{v}_b(t) - 1;$$

$v_0 = 1$ – diagram curvature parameters “ $\sigma - \varepsilon$ ”,

\hat{v}_b – coefficient of concrete elasticity at the diagram top “ $\sigma - \varepsilon$ ”,

η_d – the deformation level determined by the formula:

$$\eta_d = \frac{\varepsilon_i}{\hat{\varepsilon}_b};$$

$\hat{\varepsilon}_b$ – ultimate compression unite strain,

$$\hat{\varepsilon}_b = R_b / (E_{b0} \cdot \hat{v}_b).$$

where R_b – design concrete strength to compression at normal temperature.

The distance from the effective area to the neutral axis of the section is determined by the formula

$$Y_c = \frac{\sum_{i=1}^n S_{red,i} + \sum_{j=1}^k S'_{red,j}}{\sum_{i=1}^n A_{red,i} + \sum_{j=1}^k A'_{red,j}};$$

$$S_{red,i} = A_{red,i} \cdot \left(Y_i - \frac{h}{2 \cdot n}\right) = A_{red,i} \cdot \left(\frac{2 \cdot i - 1}{2 \cdot n}\right) \cdot h;$$

$$S'_{red,j} = A_{red,i} \cdot Y_{sj};$$

$$A_{red,i} = b \cdot \frac{h}{n} \cdot \left(\frac{f(\varepsilon_{i-1}) + f(\varepsilon_i)}{2 \cdot f(\varepsilon_0)}\right);$$

$$A'_{red,j} = A_{red,i} \cdot \frac{E_s}{f(\varepsilon_i)};$$

where

$S_{red,i}$ and $A_{red,i}$ – respectively, the static moment and the area of the *i*-th part of the section of the compressed fiber reduced to concrete,

$S'_{red,j}$ and $A'_{red,j}$ – respectively, the static moment and the area of the *j*-th woven steel mesh area reduced to the concrete compressed fiber section.

From the equilibrium condition of the element’s normal section with a simple bend it follows

$$M = \sum_{i=1}^n \left(\frac{\sigma_{i-1} + \sigma_i}{2} \right) \cdot \frac{b \cdot h}{n} \cdot \left(Y_i - \frac{h}{2 \cdot n} - Y_c \right)^2 + \sum_{j=1}^k \sigma_{sj} \cdot A_s \cdot (Y_{sj} - Y_c)^2.$$

The the cross section stiffness is determined by the formula

$$D = \frac{M}{\chi} = \frac{M \cdot h}{\varepsilon_{bt} + \varepsilon_b}.$$

Thus, by setting the relative deformation ε_{bt} and substituting the values $i = 1, 2, \dots, n, j = 1, 2, \dots, k$ in the above formulas, in each final element, the unit strain and stress can be determined, as well as the position of the neutral axis, bending moment and stiffness at any level of the considered section stress state.

A graphic illustration of the method's results and its comparison with experimental data for samples of series 1 and 3 are shown in Fig. 5.

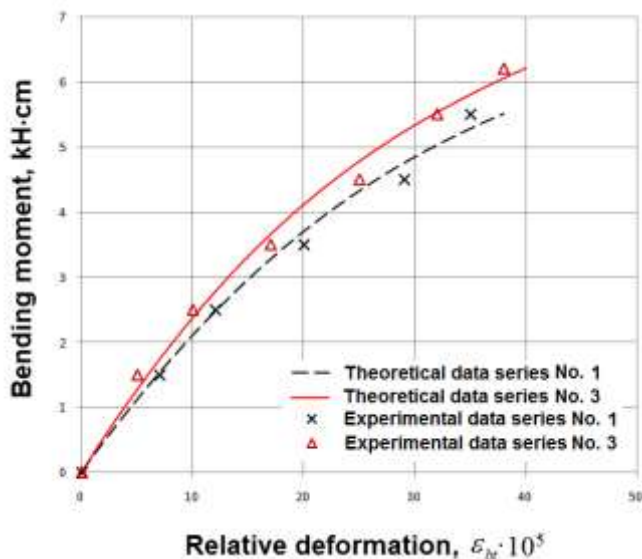


Fig. 5. The bending moment dependence on the deformation of the concrete element effective area.

IV. CONCLUSION

Thus, natural and numerical methods of research have shown that the vermiculite concrete layer increases the rigidity and crack resistance of reinforced concrete constructions. The proposed numerical method for determining the stress-strain state of a bent double-layer cement-reinforcement elements provides an acceptable match with the experimental studies results.

References

- [1] P.P. Gedonov, V.S. Spirana, "Cement-vermiculite plaster solutions for residential and public buildings", Building materials based on vermiculite, toxins and evils. Collection of works UralNIStromproekt, pp. 24–30, 1975.
- [2] K.N. Dubenetkii, A.P. Pozhnin, Vermiculite. Leningrad: Publishing House Stroyizdat, 1971, 175 p.
- [3] G.G. Nikolskii, A.P. Pozhnin, "Vermiculite and its application in construction, the All-Union Association "Knowledge"", Series building industry, vol. 13, 19 p., 1959.
- [4] T.A. Hezhev, A.V. Zhurtov, A.S. Tsipinov, S.V. Klyuev, "Fire resistant fibre reinforced vermiculite concrete with volcanic application", Magazine of Civil Engineering, vol. 80, iss. 4, pp. 181–194, 2018.
- [5] S.V. Klyuev, A.V. Klyuev, T.A. Khezhev, Y. Pukhareno, "High-strength fine-grained fiber concrete with combined reinforcement by fiber", Journal of Engineering and Applied Sciences, vol. 13, pp. 6407–6412, 2018.
- [6] I.A. Isakov, "Application of the "Deformation Model of a Section" for the calculation of reinforced concrete beams", Bulletin of Civil Engineers, vol. 32, no. 3, pp. 119–122, 2012.
- [7] V.N. Bondarenko, V.I. Kolchunov, Design models of reinforced concrete power resistance. Moscow: ASV Publishing House, 2004, 472 p.
- [8] S.V. Klyuev, A.V. Klyuev, A.D. Abakarov, E.S. Shorstova, N.G. Gafarova, "The effect of particulate reinforcement on strength and deformation characteristics of fine-grained concrete", Magazine of Civil Engineering, vol. 75 (7), pp. 66–75.
- [9] N.I. Karpenko, General Models of Reinforced Concrete Mechanics. Moscow: Stroyizdat, 1996.
- [10] V.I. Morozov, Yu.V. Pukhareno, A.V. Yushin, "The numerical investigations of double-span concrete beams strengthened with fiber reinforced plastics across the oblique section", Materials Physics and Mechanics, vol. 31 (1–2), pp. 40–43.
- [11] A.N. Sorokin, "Calculation of the fire resistance of reinforced concrete columns with full deformation of concrete", Fire Resistance of Building Structures, vol. 8, pp. 28–33.